Distillation of a one-dimensional Bose-Einstein condensate

Agnieszka Górecka[1] and Mariusz Gajda[1,2]
[1]*Institute of Physics, Polish Academy of Sciences, al.Lotnikow 32/46, 02-668 Warsaw, Poland*
[2]*Faculty of Mathematics and Natural Sciences, College of Sciences, Cardinal's Stefan Wyszyński University, ul. Dewajtis 5, 01-815 Warsaw, Poland*
(Received 19 June 2008; published 14 May 2009)

We study the dynamics of a one-dimensional Bose-Einstein condensate located in a time-dependent double-well trapping potential. In particular we investigate the way the system discovers existence of a ground state created in the new deeper well. It was shown that the transfer of the system into the minimum of the potential is triggered by the appearance of the condensate in the new well. Only then the thermal cloud follows the condensed part. During the transfer the eigenvectors of the single-particle density matrix have components localized simultaneously in both wells, which indicates a partial coherence between the two parts of the system.

DOI: 10.1103/PhysRevA.79.053624 PACS number(s): 03.75.Kk, 64.60.My

I. INTRODUCTION

The theory of the Bose-Einstein condensate (BEC) for weakly interacting systems at zero temperature is well established. On the other hand description of the system at nonzero temperature is a much more demanding task. There are several approaches to tackle this problem [1–5]. Studies of finite temperature effects were restricted in most cases to systems at thermal equilibrium. Description of a system which is not in thermal equilibrium is very complicated and requires a finite temperature theory which is applicable to dynamical situations. Examples of such processes studied previously are the evaporative cooling [6–8] or the dynamical instability followed by conversion of a condensate to a thermal cloud [9].

Our paper is inspired by the experiment of MIT group [10] in which authors observed a transfer of a BEC to a dynamically created deeper potential well separated from the initial one by a potential barrier, Fig. 1. We study theoretically an analogous process in a one-dimensional (1D) geometry. This is a serious difference as compared to [10] and therefore our results and interpretation should not be automatically extended to the three-dimensional (3D) systems as studied in [10].

Our goal is to theoretically investigate the distillation process in 1D system. Despite of relatively simple geometry this is quite complicated task as description of this process requires inevitably a finite temperature approach. We use the classical fields method [1,2] proved to be a very successful in studies of equilibrium properties of atomic condensates [11,12] as well as some dynamical phenomena such as dissipative dynamics of a vortex or decay of a doubly charged vortex [13,14]. By analyzing a temporal structure of the single-particle density matrix we are able to get a deep insight into all essential processes responsible for the atomic transfer. This way we can investigate many aspects of the quantum flow in a search for the true thermal equilibrium.

In Sec. II we briefly introduce the classical field approximation and in Sec. III describe our model. In Sec. IV we present results of simulations and distinguish various stages of the atom flow, while in Sec. V we focus at details of these stages and explain the transfer mechanism. We summarize the results of this paper in Sec. VI.

II. SUMMARY OF THE CLASSICAL FIELDS METHOD

The main idea of the classical fields method is to substitute *all* annihilation (and creation) operators of atoms, for states that occupation is significant, by c-number amplitudes and to neglect a small remaining high-energy part. This way the whole system, a condensate and a thermal cloud, is described by a single classical field, $\psi(\mathbf{r},t)$. The classical fields method is a generalization of the Bogoliubov approach to finite temperatures. The time evolution of the classical field at a finite temperature is given by the standard Gross-Pitaevskii equation as follows:

$$i\hbar\partial_t\psi(\mathbf{r},t)=\left(-\frac{\hbar^2}{2m}\triangle+V(\mathbf{r})+gN_{\mathrm{at}}|\psi(\mathbf{r},t)|^2\right)\psi(\mathbf{r},t), \quad (1)$$

where $\hbar$ is the Planck constant, m is the mass of the atom, $V(\mathbf{r})$ is the external potential, N_{at} is the number of particles in the system, and g determines the interaction strength. The nonlinear parameter g is related to the two-body scattering length a_s by the following formula:

$$g=\frac{4\pi\hbar^2 a_s}{m}. \quad (2)$$

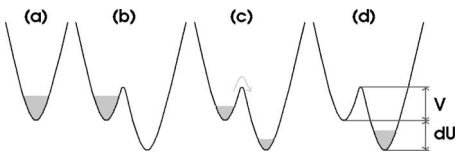

FIG. 1. The distillation of a condensate in a double-well potential. (a) A condensate is loaded into the single-well potential. (b) The potential is linearly transformed from a single-well to a double-well potential. (c) Atoms travel from the left to the right well. (d) The final equilibrium state is reached. Double-well potential can be characterized by two parameters: the difference between the wells depth dU and the height of the potential barrier V, measured from the bottom of the left well. The barrier height is significantly higher than the peak atomic mean-field energy.

There are however two important modifications as compared to the zero-temperature Bogoliubov approach. First, the initial energy of the system, conserved in the evolution, has to be larger than the energy of the ground state. Therefore the initial state evidently corresponds to a temperature greater than zero. The second important difference is that the equation Eq. (1) has to be solved on a finite grid with Δ_r being a spatial step [15]. This step defines a maximal momentum taken into account in the dynamical equation. We will refer to this momentum as to the cut-off momentum $k_{\max}=\pi/\Delta_r$. For a uniform system the number of spatial grid points equals to a number of plane waves included in the evolution (in this case plane waves are natural eigenmodes of single-particle density matrix). All plane waves included are classical if we choose the number of atoms to be

$$N_{\mathrm{at}}n_c = 1, \tag{3}$$

where n_c is the smallest eigenvalue of the single-particle density matrix as defined below, Eq. (5). Knowing the numerical value of n_c one can obtain the value of the total number of particles $N_{\mathrm{at}}=1/n_c$ in the system. The number of particles and temperature are not control parameters of the classical fields method. In numerical implementation one controls a total energy, a number of classical modes, and a value of the product gN_{at}. The actual values of particle number N_{at} and interaction strength g are determined *a posteriori* from condition Eq. (3). The cutoff has to be chosen carefully accordingly to the system energy [16,17].

The nonlinear dynamics of the high-energy classical field drives the system to the state of a thermal equilibrium [1,4,6] characterized by the equipartition of energy. Splitting the system into a condensate and a thermal cloud is based on the analysis of the time-averaged single-particle density matrix,

$$\rho(\mathbf{r}_1,\mathbf{r}_2) = \frac{1}{\Delta t}\int_t^{t+\Delta t} \psi^*(\mathbf{r}_1,\tau)\psi(\mathbf{r}_2,\tau)d\tau. \tag{4}$$

The averaging procedure reflects a real observation process and finite resolution of detectors. The averaging procedure brings the classical field to the mixed state. Diagonalization of the averaged density matrix

$$\rho(\mathbf{r}_1,\mathbf{r}_2) = \sum_i^{i_{\max}} n_i\phi_i^*(\mathbf{r}_1)\phi_i(\mathbf{r}_2) \tag{5}$$

gives one-particle orbitals $\phi_i(\mathbf{r})$ and their relative occupations n_i. The most populated mode is a condensate while all others contribute to a thermal cloud.

The analysis described above can be simplified in the case of a uniform system with periodic boundary conditions because eigenstates of single-particle density matrix are plane waves. This is not the case in the problem studied here—the potential has no translational symmetry. In numerical simulations we apply the split-step method based on Fourier decomposition; therefore we still use the plane-wave basis. The cutoff is defined in the momentum space—we neglect all states of momenta larger than cutoff. The cutoff is properly chosen if all macroscopically occupied modes are well reproduced by a superposition of the plane waves used in the numerical simulations. Evidently some nonclassical states have nonvanishing projection on the subspace spanned by the plane waves used. Due to these states some extremely small eigenvalues must appear in the spectrum of a single-particle density matrix of an equilibrium state. Fortunately the number of these states is small as compared to the total number of basis functions. These eigenfunctions must be ignored in the final analysis.

The spectrum of the single-particle density matrix of nonuniform system has the following general structure: (i) one dominant eigenvalue equal to the relative occupation of the condensate N_0/N_{at}, (ii) a wide plateau of small eigenvalues corresponding to relative occupations of different thermal states, sum of all these eigenvalues gives thermal fraction, (iii) few extremely small eigenvalues which must be neglected as they correspond to nonclassical states (see Fig. 3). In practical applications the cut-off momentum corresponds to the end of the plateau part of the spectrum and this "cut-off" eigenvalue is used to define a number of particles: $N_{\mathrm{at}}=1/n_c$. This way the absolute occupation of all states up to the cutoff is macroscopic. Previous studies show that such choice of cutoff correctly reproduces many experimental observations for instance it gives a correct estimation of the critical temperature [12].

The classical fields method allows to assign single-particle energies to each eigenstate of $\rho(\mathbf{r}_1,\mathbf{r}_2)$. This energy is equal to a characteristic frequency observed in a spectrum $\tilde{a}_i(\omega)=\int e^{-i\omega t}a_i(t)dt$ of a given eigenmode amplitude $a_i(t)=\int\phi_i^*(x)\psi(x,t)dx$. In a case of homogenous gas it was shown that the single-particle energy spectrum determined from the classical field method agrees with Bogoliubov-Popov formula [2].

III. MODEL

In the simulations we model the trapping potential by a rectangular-shaped double well with smoothen edges. This shape differs from the oscillatory potential but such choice allows for an easy modification of the wells depth without changing their shape. The numerical potential describing initial trap is given by the following formula:

$$V_{\mathrm{in}} = U(x,x_1,x_2), \tag{6}$$

where $U(x,x_1,x_2)$ is the rectangular-shaped well with smoothed edges at $x_1=-2a_0$ and $x_2=-a_0$ [18] and a_0 is a characteristic size of the well, Fig. 2. The characteristic energy of the rectangular well of a size a_0 is

$$e_0 = \frac{\hbar^2}{ma_0^2} \tag{7}$$

and the typical time is

$$t_0 = \frac{\hbar}{e_0} = \frac{ma_0^2}{\hbar}. \tag{8}$$

We choose the spatial extension of the initial well to be equal to $a_0=12\ \mu$m. This is the unit of length in our calculations. Corresponding energy unit equals $e_0=0.14\ \mathrm{nK}\times k_B$ and the time unit is $t_0=0.05$ s.

In our calculations we made two very significant assumptions which are: (1) 1D geometry of the system and (2) a

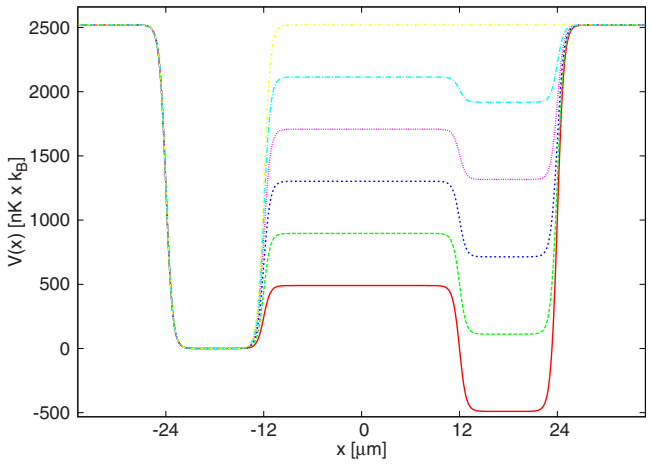

FIG. 2. (Color online) The potential at various times of the transformation, from the top to the bottom: $0t_0(0s)$, $2t_0(0.1s)$, $4t_0(0.2s)$, $6t_0(0.3s)$, $8t_0(0.4s)$, and $10t_0(0.5s)$. The time of the transformation is $t_t=10t_0$. The height of the barrier changes from $18000e_0(2520\ \mathrm{nK}\times k_B)$ to $3500e_0(490\ \mathrm{nK}\times k_B)$ and the depth of the right well changes from $18000e_0(2520\ \mathrm{nK}\times k_B)$ to $-3500e_0(-490\ \mathrm{nK}\times k_B)$.

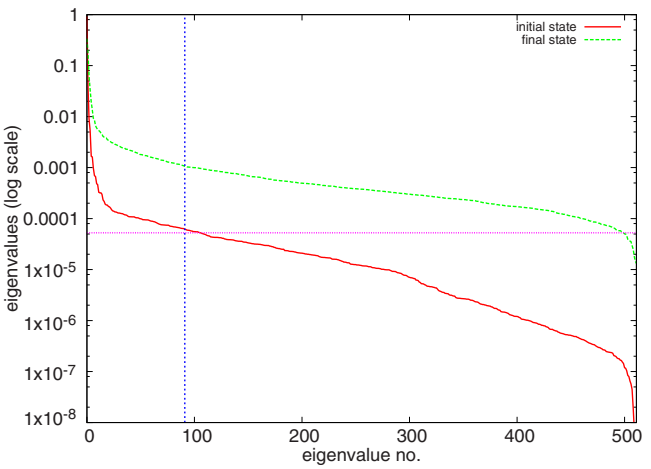

FIG. 3. (Color online) The relative occupation of the initial (solid line) and final (dashed line) single-particle orbitals. The horizontal line shows the population cutoff for the final state. The vertical line shows the number of macroscopically occupied orbitals in the initial state. We use the logarithmic scale. The initial state was created in the single-well potential. Trap parameters for the final state are $V_b=3500e_0(490\ \mathrm{nK}\times k_B)$ and $V_r^f=-3500e_0(-490\ \mathrm{nK}\times k_B)$.

semirectangular shape of the trap. These simplifications make our work quite far from the experiment [10]. Therefore many aspects of the transfer may be different in 1D and in 3D geometries.

To make some estimations let us notice that the above barrier transfer is possible only when the atoms get excited. Excitation dynamics depends on the shape of the trapping potential. In particular all levels in the harmonic trap, as used in [10], are equally spaced and for the radial and axial frequencies ($f_r=830$ Hz, $f_z=12.4$ Hz) the energies of single excitations are 36 $\mathrm{nK}\times k_B$ and 0.6 $\mathrm{nK}\times k_B$, respectively. In our rectangular-shape trap the distances between energy levels vary depending on the energy. The energy of excitation from the ground state is 5 $\mathrm{nK}\times k_B$ but the energy needed for the excitation from the state located at the top of the barrier is 70 $\mathrm{nK}\times k_B$. Excitations energies in our rectangular trap are much larger (by a factor of 100) than in the harmonic trap. Therefore, we predict that the time scales of the observed processes in our model should be about two orders of magnitude larger than in the experiment [10].

The potential is transformed in time according to the formula

$$V(t) = U(x,x_1,x_2) + a(t)U(x,x_3,x_4) - b(t)U(x,x_2,x_3), \quad (9)$$

where $x_3=a_0$ and $x_4=2a_0$ are the edges of the right well and x_2 and x_3 are the edges of the barrier. Parameters $a(t)$ and $b(t)$ determine the depth of the right well and the height of the barrier correspondingly. Both parameters are ramped linearly during the potential transformation. The final depth of the right well is $V_r^f=-3500e_0$ and the final height of the barrier varies from $2600e_0$ to $3500e_0$ (Fig. 2). All energies are measured with respect to the bottom of the left well. The time of the potential transformation is equal to $t_t=10t_0$ and is longer than the characteristic time of the nonlinear dynamics $(1/gN_{\mathrm{at}})$.

The dynamics of the system is governed by 1D version of Eq. (1). We choose the value of $G=gN_{\mathrm{at}}$ [19] such that the chemical potential of the system in the ground state of the initial well is below of the final barrier height.

The initial state was created by a random perturbation of the ground state of the initial trap followed by a thermalization. We make sure that the system reaches a state of the thermal equilibrium by comparing the relative occupations of single-particles orbitals at different moments of time evolution. The equilibrium is reached if the mean occupations do not change. The energy of the initial state is $E_i=1580.3e_0$ which is about 20% higher than the energy of the ground state. The largest eigenvalue of the time-averaged density matrix gives relative occupation of the condensate. In this case the initial state contains about 92% of condensed atoms. The remaining atoms form a thermal cloud and occupy other eigenstates of the single-particle density matrix (Fig. 3, solid line).

The essence of the classical fields method is to account in numerical simulations for macroscopically occupied modes only. In a thermal equilibrium number of macroscopically occupied modes does not depend on time. However it is not the case in the problem studied here. After transformation of the potential the system reaches a new equilibrium corresponding to a higher than the initial temperature. Therefore evidently the number of macroscopically occupied modes increases. There are two ways to solve this issue: to change dynamically the number of classical modes (it corresponds to changing the number of the grid points) or to adjust the number of the classical modes to the final temperature. We choose the second strategy allowing for some nonclassical modes in the initial state.

Figure 3 shows the relative populations of single-particle orbitals for the initial (solid line) and the final state (dashed line). The chosen population cutoff is marked by a horizontal

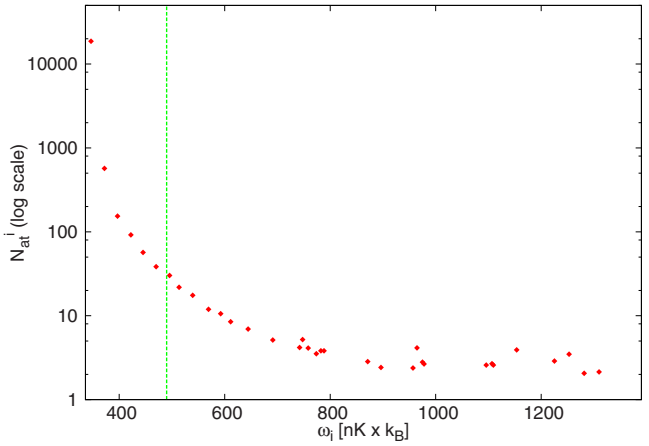

FIG. 4. (Color online) Number of atoms in a given orbital as a function of a corresponding energy. The vertical line shows the barrier height $V_b=3500e_0(490\ \text{nK}\times k_B)$. The total number of atoms in the system is $N_{\text{at}}=2\times10^4$. We use the logarithmic scale.

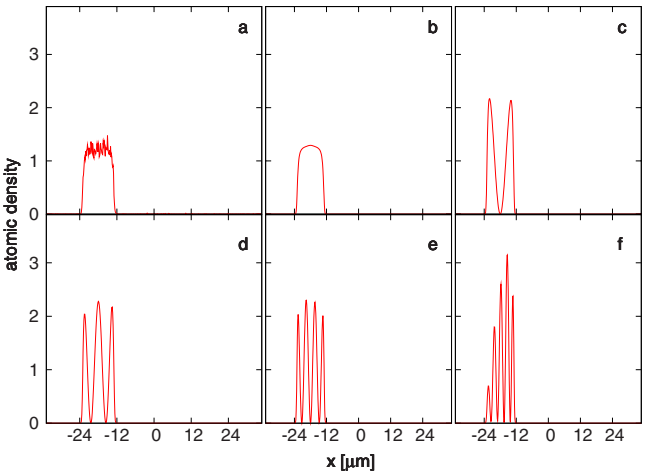

FIG. 5. (Color online) The atomic density (a) and the eigenvectors (b)–(f) of the initial state as a function of position. The well is localized between $x_1=-2a_0(-24\ \mu\text{m})$ and $x_2=-1a_0(-12\ \mu\text{m})$, as shown in Fig. 2. The occupation of the eigenstates is the following: (b) $n_0=92.56\%$, (c) $n_1=3.84\%$, (d) $n_2=0.90\%$, (e) $n_3=0.53\%$, and (f) $n_4=0.4\%$. All eigenstates are localized in the left well.

line in Fig. 3. All states of occupation larger than determined by the horizontal line are classical. According to our discussion in Sec. II this choice of the cutoff gives the total number of atoms equal to $N_{\text{at}}=2\times10^4$ at final equilibrium. However for such number of particles only the first 91 eigenstates of the *initial* single-particle density matrix have occupations larger than one. This is indicated by a vertical line in Fig. 3. For other initial eigenstates the classical approximation is not justified. As we already mentioned these nonclassical states are considered because they will became classical in further evolution. One can ask a legitimate question how it will affect the dynamics of the system.

Transfer of atoms to empty (nonclassical) states is due to the spontaneous process only. These are not accounted for in the classical fields method, which includes only stimulated processes. For this reason transfer of atoms to these nonclassical states cannot be correctly described what affects a total time of reaching a thermal equilibrium but has not significant impact on the dynamics of the transfer of atoms from the initial to the final minimum of the potential. In Fig. 4 we plot the occupation of low-energy states. The vertical line indicates the final energy of potential barrier separating both potential minima. Only the first seven states have the energy below the barrier. All other states have larger energy. A population of these states is macroscopic (larger than five atoms per state) and transfer of particles to these states is totally dominated by stimulated processes. This way one can see that the transport of atoms to the new equilibrium can be well described by the classical modes of the system. We believe that our calculations give the correct description of the transfer of atom to the minima in 1D system but they probably fail in final stages of thermalization process. Figure 5 shows the atomic density and some eigenvectors of the initial state. The initial state is localized in the left well.

IV. RESULTS

Below we present results of our numerical simulations. The total time of the evolution (after transformation of the potential) is $t_e=10\ 000t_0$.

In the simulations the single-particle density matrix was averaged over a very short time (as compared to the typical time scale of the dynamics), $\Delta t=0.1t_0$, which is about 5 ms. The longer time of averaging does not change the spectrum of the density matrix.

A time after which the condensate is transferred into the right well can be estimated by monitoring the potential energy

$$E_V=\int \psi^*(x,t)V(x)\psi(x,t)dx, \tag{10}$$

where $V(x)$ is the trapping potential. When particles appear in the right well the potential energy drops significantly. In Fig. 6 we show the potential energy as a function of time for different final barrier heights. A drop of the potential energy is clearly visible. This abrupt drop of energy is accompanied by a macroscopic transfer of atoms to the new well. In the inset of Fig. 6 we show the transfer time for different values of the potential barrier. For larger values of V_b the transfer time increases linearly. The transfer cannot be attributed to the tunneling. The tunneling rate is given by the formula

$$R=\frac{\mu}{\hbar}\exp\left[-\sqrt{\frac{2md^2(V_b-\mu)}{\hbar^2}}\right], \tag{11}$$

where d is the barrier width. The tunneling time for $V_b=2600e_0$ is $t_{\text{tun}}=1/R=0.5\times10^{12}t_0$ and for $V_b=3500e_0$ it is $t_{\text{tun}}=0.33\times10^{21}t_0$. Such time scales are by orders of magnitude larger than any reasonable time scales; therefore the tunneling effects are irrelevant in the studied process.

Fraction of atoms localized in three different spatial regions: right well, left well, and the barrier as a function of time is shown in Fig. 7. We estimate the relative number of particles in a given region using the following formula:

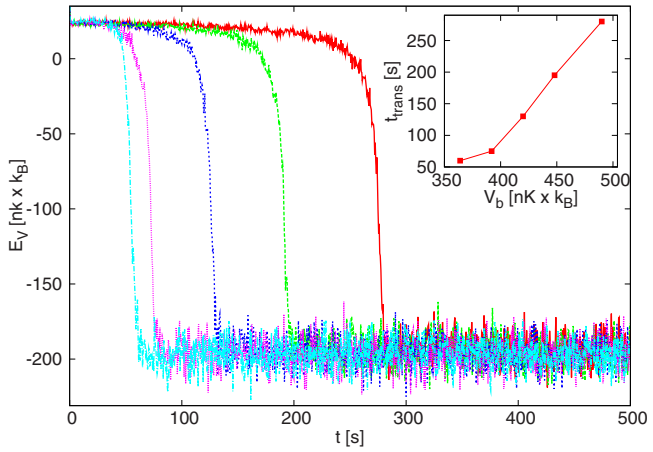

FIG. 6. (Color online) The value of the potential energy as a function of time for different final barrier heights. Final barrier heights are (from the most left to the right): $V_b=2600e_0(364\ \mathrm{nK}\times k_B)$, $V_b=2800e_0(392\ \mathrm{nK}\times k_B)$, $V_b=3000e_0(420\ \mathrm{nK}\times k_B)$, $V_b=3200e_0(448\ \mathrm{nK}\times k_B)$, and $V_b=3500e_0(490\ \mathrm{nK}\times k_B)$. In the inset we show the transfer time as a function of the barrier height. The right well depth was $-3500e_0(490\ \mathrm{nK}\times k_B)$.

$$N_{\mathrm{at}}^{\mathrm{loc}}=\int_{x_i}^{x_f}\psi^*(x,t)\psi(x,t)dx, \tag{12}$$

where x_i and x_f are the edges of the examined area (left and right wells or barriers). This formula overestimates the number of particles trapped in each well because of contribution of atoms of energies higher than the barrier height which oscillate inside the whole trap.

Let us notice that the sudden drop of the potential energy (Fig. 6) is accompanied by a significant transfer of atoms to the new well. At the final stage of the dynamics the number of atoms in the barrier area is the same as the number of atoms in the initial well. In Fig. 8 we show a fraction of condensated atoms (the lowest-energy state in each well) in the left and right wells. The condensate populations are normalized to the number of atoms localized in corresponding well. In particular the normalization is different for both wells. The condensate fraction is a measure of the temperature in each part of the system—the larger the condensate fraction the smaller the temperature is.

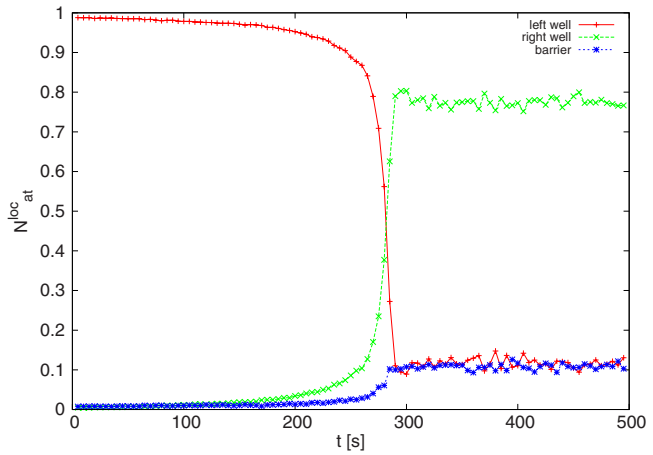

FIG. 7. (Color online) The fraction of atoms in the left well, in the right well, and in the barrier during the evolution. The final barrier height is $3500e_0(490\ \mathrm{nK}\times k_B)$ and the final depth of the right well is $-3500e_0(490\ \mathrm{nK}\times k_B)$.

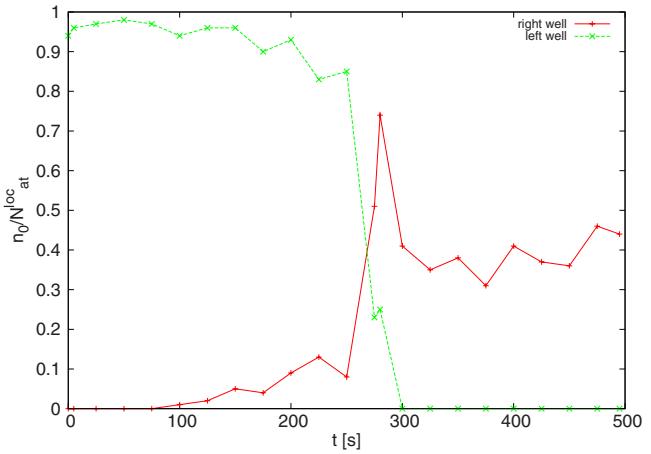

FIG. 8. (Color online) Number of atoms in the ground state of the left and the right wells normalized to the total number of atoms in the left and the right wells, respectively. Note that $N_{\mathrm{at}}^{\mathrm{loc}}<1$ and n_0 is smaller than $n_0/N_{\mathrm{at}}^{\mathrm{loc}}$. The final barrier height is $3500e_0(490\ \mathrm{nK}\times k_B)$ and the final depth of the right well is $-3500e_0(490\ \mathrm{nK}\times k_B)$.

Figure 8 suggests that one can distinguish three different stages of the system evolution. Initially, when all atoms are trapped in the left well the temperature very slowly increases and the condensate fraction decreases to the value of 80% at time $5000t_0$. Within the next 1000 time units the condensate completely evaporates from the initial well and appears in the dynamically created deeper well. Then, in the third stage, the system is slowly approaching a state of the thermal equilibrium and the condensate fraction at the end of our simulations is about 40% ($t=10000t_0$).

In the experiment [10] the same quantities were monitored. On the first glance we see some qualitative similarities; however our analysis does not allow to judge whether the distillation scenarios in the studied 1D model and in the 3D geometry as in [10] are analogous or not. In many cases a 1D and a 3D physics of a Bose-Einstein condensates is different [20]. At least one difference can be expected on the basis of the previous discussion (Sec. III): the time scale of the transfer is about 100 times larger than in the experiment [10]. The other difference is that in our calculations one can see the prominent peak in the fraction of condensated atoms in the right well immediately after the transfer. Only later the condensate fraction decreases. It would be interesting to check whether this result is specific to the 1D geometry or if it is of a more general character. The ultimate test would be the experiment with a high temporal resolution.

V. DISTILLATION SCENARIO

In this section we present details of the transfer of atoms to the dynamically created ground state and show how the system finds its way toward a new equilibrium. All following

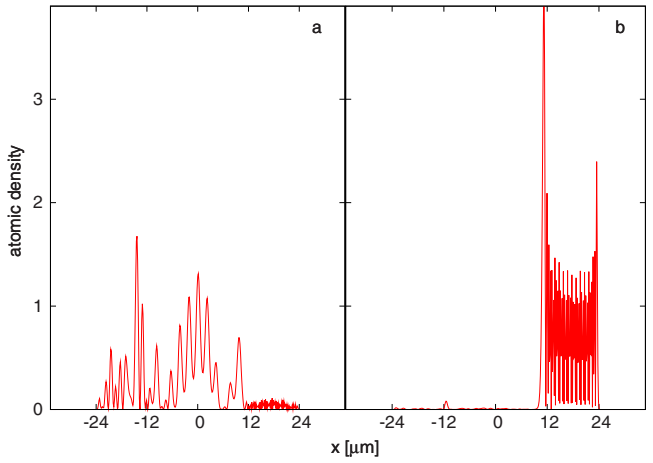

FIG. 9. (Color online) Some single-particle orbitals as a function of position at $t=200t_0(10s)$. The relative occupation of the states is: (a) $n_5=0.07\%$ and (b) $n_{25}=0.02\%$. Final barrier height is $3500e_0(490\ \mathrm{nK}\times k_B)$ and final depth of the right well is $-3500e_0(490\ \mathrm{nK}\times k_B)$.

results are for the final barrier height equal to $3500e_0$ and the final depth of the right well equal to $-3500e_0$.

A. Penetrating a potential minimum

After the transformation of the trapping potential the system is no longer at the thermal equilibrium. Until time $5000t_0$ (250 s) the system remains in the initial well. Atomic density practically does not change. However, populations of different eigenvectors of the single-particle density matrix change in time.

For a relatively short time $t=200t_0$ (10 s) the whole system is practically localized in the initial well. All single-particle states look very similar to the eigenstates at the thermal equilibrium. However, we observe a migration of population toward higher energy states of the left well. For example, a population of the first-excited state is equal to $n_2=0.22\%$ and is larger than population of sixth-excited state $n_3=0.12\%$. However populations of the third-, fourth-, and fifth-excited states are smaller than the population of the sixth state. This is a signature of a population inversion. Simultaneously a few thermal atoms penetrate the whole region of the double-well potential [Fig. 9(a)]. There is already a tiny fraction of atoms (about 0.02%) trapped in the high-energy states of the right well [Fig. 9(b)].

At time $t=3500t_0$ (175 s) the condensate rests in the initial minimum and its population is close to the initial value (about 90%). Simultaneously a small thermal fraction is trapped in the new minimum. While population still climbs up the energy levels in the first minimum the opposite happens in the new well—the population travels toward the low-energy states. The true ground state of the system [Fig. 10(b)] has already noticeable occupation $n_{14}=0.12\%$. There are however higher-energy states of larger occupancy, for example: $n_{12}=0.13\%$ [Fig. 10(a)]. The first-excited state in the new well has still relatively low occupation: $n_{39}=0.04\%$ [Fig. 10(c)].

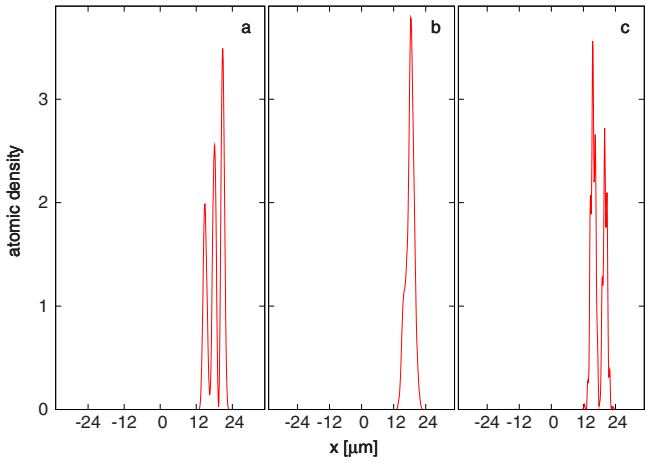

FIG. 10. (Color online) Some single-particle orbitals as a function of position at $t=3500t_0(175s)$. The occupation of the eigenstates is following: (a) $n_{12}=0.13\%$, (b) $n_{14}=0.11\%$, and (c) $n_{39}=0.04\%$. The new condensate starts to form in the right well. Final barrier height is $3500e_0(490\ \mathrm{nK}\times k_B)$ and final depth of the right well is $-3500e_0(490\ \mathrm{nK}\times k_B)$.

B. Rapid transfer

The rapid transfer of atoms to the new minimum starts around $t=5000t_0$—Fig. 12. The total transfer time is about $1000t_0$, which is only 10% of the total time of penetration of the potential minimum.

At $t=5500t_0$ (275 s) the system can be perceived as composed of two coupled macroscopic subsystems: one localized in the left well [its eigenstates are shown in Figs. 11(a) and 11(c)] and second localized in the right well [Figs. 11(b) and 11(d)]. Occupations of both wells are comparable. The lowest-energy states in each well form two separated condensates. The occupations of these condensates are similar: for the left well it is about $n_0=16\%$ and for the right well it is $n_1=12\%$.

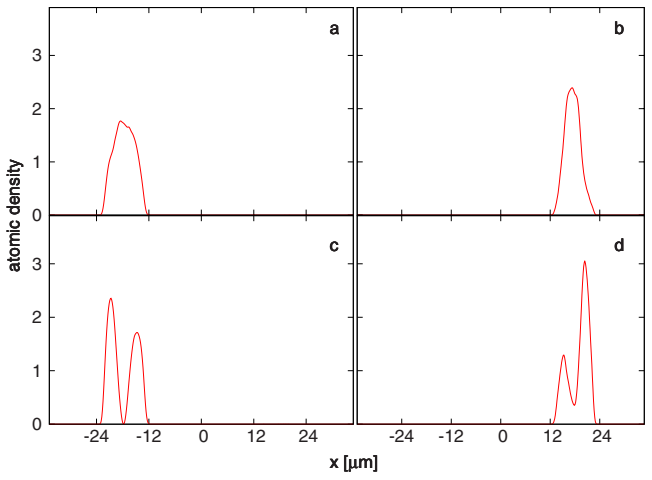

FIG. 11. (Color online) Some single-particle orbitals as a function of position at $t=5500t_0(275s)$. The occupation of the eigenstates is: (a) $n_0=16.1\%$, (b) $n_1=11.92\%$, (d) $n_2=9.53\%$, and (c) $n_3=7.43\%$. Notice two separate condensates in the left and right well. Final barrier height is $3500e_0(490\ \mathrm{nK}\times k_B)$ and final depth of the right well is $-3500e_0(490\ \mathrm{nK}\times k_B)$.

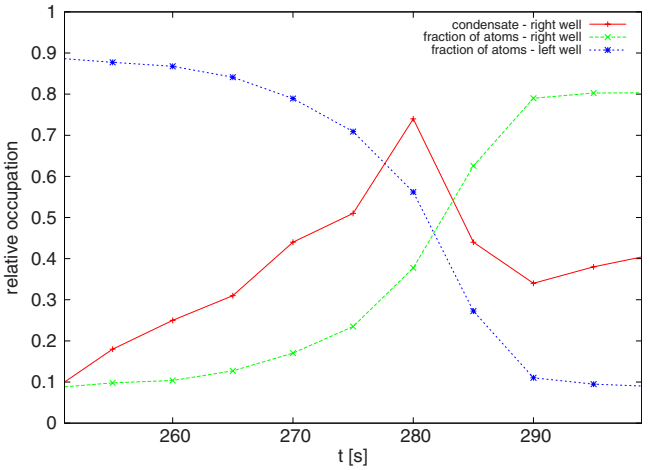

FIG. 12. (Color online) Transfer of the condensate and the thermal cloud. Solid line shows the relative occupation of condensate in the right well normalized to the fraction of atoms in this well. Dashed line shows the fraction of atoms in the right well and doted line shows the relative number of atoms in the left well. Final barrier height is $3500e_0(490\ \mathrm{nK}\times k_B)$ and final depth of the right well is $-3500e_0(490\ \mathrm{nK}\times k_B)$.

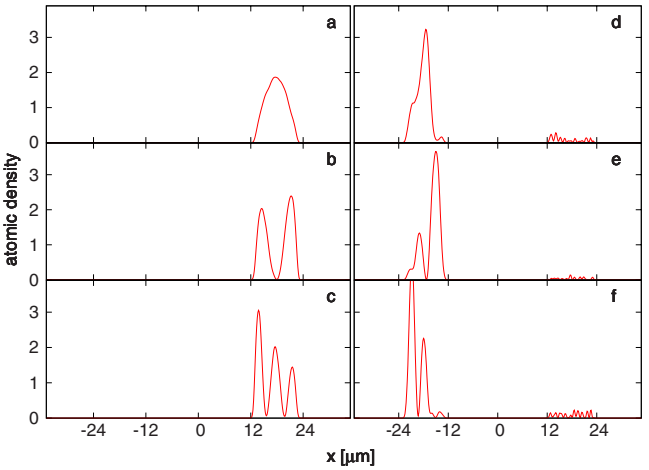

FIG. 13. (Color online) Chosen low-energy eigenstates as a function of position at $t=5600t_0(280s)$. Occupations of the eigenstates are: (a) $n_0=28.2\%$, (b) $n_1=13.75\%$, (c) $n_2=6.85\%$, (d) $n_8=1.23\%$, (e) $n_7=1.47\%$, and (f) $n_{11}=0.93\%$. Note that three lowest states of the initial well (right panel) have some fast oscillating components in the area of the minimum. Final barrier height is $3500e_0(490\ \mathrm{nK}\times k_B)$ and final depth of the right well is $-3500e_0(490\ \mathrm{nK}\times k_B)$.

At the time $t=5000t_0$ when the transfer starts there is about 10% of atoms localized in the area of the new well. Only 10% of these atoms occupy the ground state of the right well and form a "new" condensate. This is the starting point of a sudden transfer of atoms. Almost all atoms which travel into the right well feed the condensate, not the thermal cloud (Fig. 12). One must notice that the transfer of atoms to the right well ends at the same time when condensate fraction reaches maximum in this well (Fig. 12). Our estimation of a fraction of condensed atoms in the new well immediately after the sudden transfer, $t=5600t_0$ (280 s), gives the value of about 75%. At time $t=6000t_0$ (300 s) the condensate fraction diminishes to the value of 40%.

In the classical distillation scenario one would expect that the atoms which travel into the area of the new well are thermal and only later their thermalize and the condensate is formed. In the studied case we see something opposite, an injection of the condensate from the left to the right well which resembles the famous fountain effect known from the liquid-helium experiments [21–24]. This effect is of a quantum character and indicates a kind of a coherent flow of the condensate. We find this effect as one of the most intriguing results of our paper. Experimental verification of our prediction of the coherent injection of the condensate to the new minimum in 1D would be the ultimate test of our model.

C. Reaching equilibrium

The rapid transfer of atoms stops at $t=5600t_0$ (280 s) and almost all atoms are localized in the new well at this time. The condensate fraction drops significantly as the system thermalizes.

After the transfer there are no eigenvectors localized exclusively in the initial left well. The first three eigenvectors of the density matrix are shown in Figs. 13(a)–13(c) (left panel). These are states localized in the area of the true minimum. Occupation of the condensate is about $n_0=28\%$ of total number of atoms. The three first states which remain in old minimum are shown in the right panel of Fig. 13. They have very small occupations (about 1% each) and moreover, each of them has a small component located in the right well. These vectors are still in the transient regime and are slowly "leaking" into the right well.

Finally at the time $t=9900t_0$ (495 s) most of atoms are localized in the right well [Fig. 14(a)]. The occupation of the condensate is $n_0=34\%$. All eigenstates of non-negligible occupation are localized in the right well [Figs. 14(b)–14(f)].

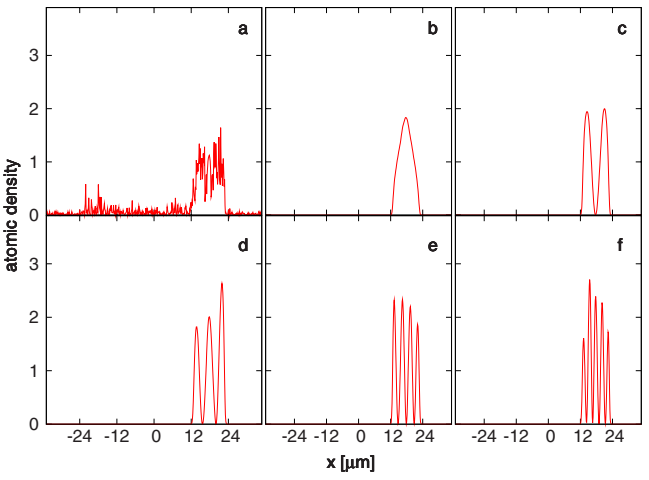

FIG. 14. (Color online) The atomic density (a) and eigenstates as a function of position at $t=9900t_0(495s)$. The occupation of the eigenstates is following: (b) $n_0=33.85\%$, (c) $n_1=17.04\%$, (d) $n_2=6.02\%$, (e) $n_3=3.36\%$, and (f) $n_4=1.94\%$. The relative occupation is normalized to N_{at}. Final barrier height is $3500e_0(490\ \mathrm{nK}\times k_B)$ and final depth of the right well is $-3500e_0(490\ \mathrm{nK}\times k_B)$.

The small fraction of atoms penetrates the whole trap. The system is close to the thermal equilibrium.

VI. SUMMARY

In this paper we study the transfer of 1D Bose-Einstein condensate, initially in the state of a thermal equilibrium, to a position where a new deeper potential minimum was dynamically created. We applied the classical fields method. We have shown that for studied geometry the distillation process is of quantum nature. It can be divided into three stages. First, after modification of the external potential the system starts to seek for a new equilibrium. Populations of higher excited states increase. Some thermal atoms of energies larger than the potential barrier do appear. Only then they start to penetrate the new minimum. Some of the atoms are trapped in the new well and then start to migrate down the energy states in the new well. This way after quite a long time the ground state of the new well becomes populated. At some moment population of this state dominates over populations of other states in the well what triggers a rapid transfer of the condensate to the potential minimum. It is unexpected that originally a great majority of atoms which escaped from the old well do appear in the lowest-energy state of the new well. It looks like the condensate from old well is being injected to the ground state of the new well. Finally, due to thermalization the condensate partially evaporates at the expense of the thermal cloud. This rapid transfer of atoms resembles the famous fountain effect observed in a liquid helium ^{4}He. Our results indicate that the studied 1D distillation process is of a quantum nature. We believe that the quantum nature of the flow can be verified in the experiment by the detection of the condensate fraction immediately after the transfer of atoms to the new well.

ACKNOWLEDGMENTS

The authors acknowledge support by the Polish Government Research Funds for 2006-2009.

[1] K. Góral, M. Gajda, and K. Rzążewski, Opt. Express **8**, 92 (2001).
[2] M. Brewczyk, P. Borowski, M. Gajda, and K. Rzążewski, J. Phys. B **37**, 2725 (2004); M. Gajda and K. Rzążewski, Acta Physiol. Pol. **100**, 7 (2001).
[3] A. Sinatra, C. Lobo, and Y. Castin, Phys. Rev. Lett. **87**, 210404 (2001); A. Sinatra, C. Lobo, and Y. Castin, J. Phys. B **35**, 3599 (2002).
[4] M. J. Davis and S. A. Morgan, Phys. Rev. A **68**, 053615 (2003); M. J. Davis and P. B. Blakie, J. Phys. A **38**, 10259 (2005).
[5] E. Zaremba, A. Griffin, and T. Nikuni, Phys. Rev. A **57**, 4695 (1998).
[6] R. J. Marshall, G. H. C. New, K. Burnett, and S. Choi, Phys. Rev. A **59**, 2085 (1999).
[7] C. W. Gardiner, P. Zoller, R. J. Ballagh, and M. J. Davis, Phys. Rev. Lett. **79**, 1793 (1997); C. W. Gardiner, M. D. Lee, R. J. Ballagh, M. J. Davis, and P. Zoller, *ibid.* **81**, 5266 (1998).
[8] D. V. Semikoz and I. I. Tkachev, Phys. Rev. Lett. **74**, 3093 (1995).
[9] A. J. Ferris, M. J. Davis, R. W. Geursen, P. B. Blakie, and A. C. Wilson, Phys. Rev. A **77**, 012712 (2008).
[10] Y. Shin, M. Saba, A. Schirotzek, T. A. Pasquini, A. E. Leanhardt, D. E. Pritchard, and W. Ketterle, Phys. Rev. Lett. **92**, 150401 (2004).
[11] K. Góral, M. Gajda, and K. Rzążewski, Phys. Rev. A **66**, 051602(R) (2002).
[12] L. Zawitkowski, M. Gajda, and K. Rzążewski, Phys. Rev. A **74**, 043601 (2006).
[13] M. Brewczyk, M. Gajda, and K. Rzążewski, J. Phys. B **40**, R1 (2007).
[14] K. Gawryluk, M. Brewczyk, and K. Rzążewski, J. Phys. B **39**, L225 (2006).
[15] Number of grid points in the simulations is $N_{\mathrm{grid}}=512$ and the spatial step is $\Delta_r=0.012a_0$.
[16] E. Witkowska, M. Gajda, and J. Mostowski, J. Phys. B **40**, 1465 (2007).
[17] L. Zawitkowski, M. Brewczyk, M. Gajda, and K. Rzążewski, Phys. Rev. A **70**, 033614 (2004).
[18] The single-well potential is: $U(x,x_1,x_2)=h[\tanh(x-x_1)-\tanh(x-x_2)]$, where h is the potential height.
[19] For 1D case $G=1.7\times10^5 e_0/a_0$, the number of atoms is $N_{\mathrm{at}}=2\times10^4$ and $g=8.5e_0/a_0$. For the 3D case $g_{3\mathrm{D}}=2.98\times10^{-3}e_0/a_0^3$.
[20] I. Bloch, J. Dalibard, and W. Zwerger, Rev. Mod. Phys. **80**, 885 (2008).
[21] R. J. Donnelly, Phys. Today **48**, 30 (1995).
[22] P. Kapitza, Nature (London) **141**, 74 (1938).
[23] J. F. Allen and A. D. Misener, Nature (London) **141**, 75 (1938).
[24] J. F. Allen and H. Jones, Nature (London) **141**, 243 (1938).